urban science

MDPI

Article

A Baseline Assessment of Residential Wood Burning and Urban Air Quality in Climate-Vulnerable Chilean Cities

Ricardo Baettig [1] and Ben Ingram [2,3,*]

[1] Facultad de Ciencias Forestales y de la Conservación de la Naturaleza, Universidad de Chile, La Pintana, Santiago 8820808, Chile; ricardo.baettig@uchile.cl
[2] Department of Interactive Visualization and Virtual Reality, Faculty of Engineering, Universidad de Talca, Talca 3460000, Chile
[3] Faculty of Energy and Applied Sciences, Cranfield University, Cranfield MK43 0AL, UK
* Correspondence: bri@utalca.cl

Abstract

This study presents a comprehensive latitudinal analysis of air particulate matter (PM) across an 1400 km pollution corridor spanning Chile's central-southern zone. We systematically analyzed $PM_{2.5}$ and PM_{10} concentrations across eight major urban centers (2014–2015), providing crucial pre-Paris Agreement baseline data for South America's most extensive air quality monitoring network. Our analysis reveals significant pollution gradients, with Coyhaique ranking one of the world's most severely polluted cities (95th percentile globally, WHO database) and demonstrating an extreme 86% fine particulate matter ratio that far exceeds international urban standards. Residential wood combustion (RWC) demonstrates systematic correlations with fine PM concentrations ($R^2 > 0.96$), suggesting RWC is the dominant pollution driver across multiple climate zones. The documented pollution patterns represent a concerning continental-scale environmental pattern, with 4900–6500 annual premature deaths directly attributable to $PM_{2.5}$ exposure-one of the highest per-capita pollution mortality rates in South America. This work provides a methodological framework applicable to mountain-valley pollution systems globally while addressing critical knowledge gaps in regional air quality science. The evidence indicates the need for urgent implementation of comprehensive wood combustion control strategies and positions this research as essential baseline documentation for both national air quality policy and international climate change assessment frameworks.

Keywords: residential wood combustion; air pollution; $PM_{2.5}$; PM_{10}; Chile; urban air quality; particulate matter

check for updates

Received: 1 September 2025
Revised: 3 October 2025
Accepted: 11 October 2025
Published: 15 October 2025

Citation: Baettig, R.; Ingram, B. A Baseline Assessment of Residential Wood Burning and Urban Air Quality in Climate-Vulnerable Chilean Cities. *Urban Sci.* **2025**, *9*, 426. https://doi.org/10.3390/urbansci9100426

Copyright: © 2025 by the authors. Licensee MDPI, Basel, Switzerland. This article is an open access article distributed under the terms and conditions of the Creative Commons Attribution (CC BY) license (https://creativecommons.org/licenses/by/4.0/).

1. Introduction

The presence of airborne particulate matter (PM), especially fine PM, has caused disproportionate impacts on human respiratory health, including asthma exacerbation, pulmonary dysfunction, cancer development and premature mortality, particularly affecting elderly populations [1–5].

In 2010, ambient particulate matter contributed to some 3.2 million avoidable deaths worldwide, in large part due to cardiovascular diseases, with approximately 223,000 deaths related to lung cancer [6]. In Chile specifically, at least 10 million of the country's 17 million people are exposed to average annual $PM_{2.5}$ concentrations exceeding 20 $\mu g\, m^{-3}$ [7–11], resulting in 4900–6500 annual premature deaths from cardiopulmonary diseases [12,13]—one of the highest per-capita pollution mortality rates in South America.

Despite this critical health burden, comprehensive studies examining pollution patterns across extensive latitudinal gradients remain scarce in South America [14]. Most regional air quality research has focused on single cities or limited metropolitan areas [15]. This research deficit is particularly pronounced for understanding how geographical and climatic factors influence particulate matter distribution across diverse topographical settings. This study aims to address this knowledge gap by conducting a comprehensive latitudinal analysis of $PM_{2.5}$ and PM_{10} variability across a 1400 km corridor spanning Chile's central-southern zone, examining seasonal and diurnal concentration patterns across eight major urban centers, and establishing through bivariate polar plots the systematic relationship between air particulate matter concentrations and their probable sources.

Atmospheric transport patterns demonstrate that 30–100 µm particles can travel 5–100 km from emission sources which depend on local wind conditions [16,17]. Coarse particulate matter (PM_{10}) originates primarily from uncontrolled combustion processes and fugitive dust emissions. Meteorological factors including wind speed, rainfall, and solar radiation critically determine air PM concentrations through their influence on dispersion processes, removal mechanisms, and atmospheric particle formation [18]. Urban vegetation characteristics also influence local air quality patterns [19], though their effects on PM dispersion in mountain-valley systems remain underexplored.

Beginning in the early 1990s, air quality in Santiago metropolitan region has been a matter of concern to the Chilean authorities. Approximately 7 million people live in this region, and most of them reside in a basin crossed by the Mapocho and Maipo rivers that form a depression surrounded by mountain ranges with no proper dispersion [20]. The southeastern Pacific subtropical high-pressure system [21] generates a pressure gradient characterized by reduced atmospheric pressure over coastal regions and the interior basin, thereby modulating regional meteorological patterns. This pressure configuration induces tropospheric subsidence within the lower atmospheric layers of the valley, establishing persistent conditions for temperature inversion [22–24].

This phenomenon, together with a surface inversion, is common in the cold season, affecting the particle dispersion in the central southern cities which are located in the Central Valley without the influence of Pacific Ocean. Furthermore, significant variations in temperature during clear winter days are often associated with subsidence inversion scenarios which reduce the mixing layer and particle dispersion height [23]. Few studies exist that outline atmospheric boundary layer dynamics across mountain-valley systems in South America, with only sparse research examining mixing layer heights in Chile, all focused exclusively on Santiago [23]. This research limitation severely constrains understanding of how topographical constraints influence pollution accumulation and transport across different latitudinal zones [25], despite evidence that mixing layer heights can be extremely low (below 200 m at night in Rancagua). Recent advances in mountain-valley pollution research [26–28] demonstrate the critical importance of boundary layer dynamics, while comprehensive studies of pollution gradients in mountainous terrain [29,30] provide methodological frameworks applicable to Chile's unique topographical setting. In the past decade, air quality concerns have expanded beyond Santiago to encompass cities throughout central and southern Chile, where consistently elevated PM concentrations occur each winter season. Previous research has identified wood biomass combustion as the primary source of airborne particle emissions throughout this corridor [31–36].

While residential wood combustion (RWC) has been recognized as a dominant emission source across multiple climate zones and urban settings, systematic quantitative analysis of RWC impacts across this geographical gradient has not been comprehensively documented. The prevalence of firewood stove use during winter throughout the central valley, an intermediate basin with the Andes to the east and the Coastal mountain range

to the west, tends to make this analysis particularly relevant. Recent research has demonstrated significant health impacts of residential wood combustion [37,38], while studies examining wood combustion's climate impacts [39] and toxic potency [40] highlight the importance of understanding RWC patterns across extensive geographical gradients.

According to the pollutant emission and transfer register (Registro de Emisiones y Transferencia de Contaminantes, RETC), firewood combustion was the principal source of fine PM emissions in the O'Higgins and Aysen regions (58.4%), followed by fugitive emission sources (31.4%), industrial emissions (9.3%), and mobile sources (0.9%) [7–11]. During the 1990s, most air pollution in central Santiago originated from vehicle emissions and small industries, yet $PM_{2.5}$ concentrations decreased by 52% between 1989 and 2000 [41] despite vehicle numbers growing at 10% annually and doubling during this period [42]. Santiago's decontamination policy significantly reduced emissions by removing polluting city buses and trucks, improving liquid fuel standards, and implementing new regulations on industrial emissions, road paving, and restrictions on fire use during land clearing [43,44]. However, the annual downward trend in $PM_{2.5}$ and PM_{10} concentrations has slowed and stabilized since 2000 [7–11].

Chile's position as having the most comprehensive and sophisticated monitoring network for air quality in South America [7–11] provides an unprecedented opportunity to conduct the first comprehensive latitudinal pollution assessment in the region. This unique monitoring infrastructure enables systematic analysis that would be impossible in other South American nations lacking comparable data coverage and quality.

The 2014–2015 period represents a critical baseline for understanding pollution patterns across central and southern Chile, coinciding with the initial implementation of national air quality improvement strategies and providing essential pre-Paris Agreement data for one of South America's most comprehensive pollution monitoring networks [45]. This temporal framework establishes crucial reference conditions against which current and future mitigation efforts can be evaluated, which is particularly valuable given the subsequent acceleration of climate-related air quality challenges and evolving residential heating practices throughout the region. Historical baseline data has proven essential for understanding air pollution trends [46,47], with baseline period selection critically affecting climate and pollution impact quantification [48]. The COVID-19 pandemic has further intensified residential energy consumption patterns, particularly affecting biomass use [49], making pre-pandemic baseline data increasingly valuable for understanding normal pollution patterns.

2. Materials and Methods

2.1. Data Collection

The data used in this study was downloaded in ASCII format from the SINCA network belonging to the Chilean Ministry of the Environment, which was open source data (http://sinca.mma.gob.cl/, (accessed on 10 October 2025)). The more reliable monitoring stations are located in the main urban habitats of Chile and record both PM and meteorological data, including mean daily temperature (°C), mean daily wind speed ($m\,s^{-1}$), minimum daily temperature (°C), maximum daily temperature (°C), and mean daily relative humidity (%). Recent advances in sub-hourly precipitation monitoring [50] and rainfall intensity data recovery [51] in central Chile provide complementary meteorological context for understanding PM dispersion patterns. For this article, 8 quality monitoring stations were selected out of the 53 located from central Santiago to the south of Chile, based on the relative importance of the city according to the urban habitat they represent and their location in the central valley, which is away from the direct influence of the ocean. Since there is more than one monitoring station in several cities, the chosen stations were the ones

possessing the most complete dataset. The data recorded hourly and the local time (UTC-4). Below, Table 1 and Figure 1 summarize the relevant characteristics and geographical situation of the 8 cities under study, including whether the city exceeds current regulations for PM_{10}, $PM_{2.5}$, or both.

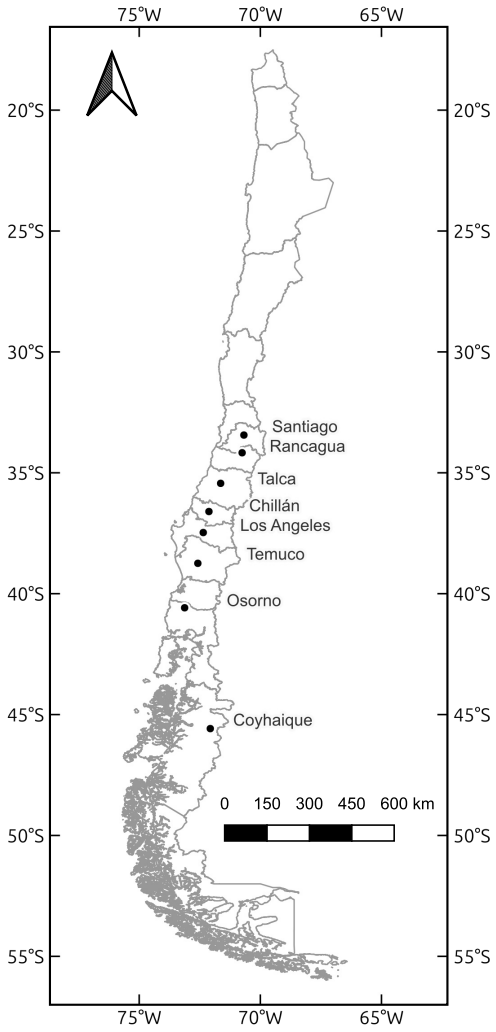


Figure 1. Map of Chile showing the location of the 8 cities under study.

Table 1. General characteristics of the 8 cities under study.

City	Santiago	Rancagua	Talca	Chillan	Los Angeles	Temuco	Osorno	Coyhaique
Abbreviation	STG	RAN	TAL	CHI	LAN	TEM	OSO	COY
Latitude	33°27′48.47″ S	34°9′43.96″ S	35°26′6.50″ S	36°36′58.25″ S	37°28′16.20″ S	38°44′55.39″ S	40°35′4.20″ S	45°34′47.91″ S
Longitude	70°39′41.15″ W	70°42′50.15″ W	71°40′41.69″ W	72°5′35.01″ W	72°21′41.50″ W	72°37′14.83″ W	73°7′7.41″ W	72°3′40.13″ W
Elevation (masl)	526	513	99	129	137	106	52	341
Exceeds	PM_{10}, $PM_{2.5}$	PM_{10}	PM_{10}	PM_{10}, $PM_{2.5}$	PM_{10}, $PM_{2.5}$	PM_{10}, $PM_{2.5}$	PM_{10}, $PM_{2.5}$	PM_{10}, $PM_{2.5}$
Köppen climate	Csb	Csb	Csb	Csb	Csb	Cfb	Cfb	Cfc

Csb—Warm temperate with winter rains (Mediterranean climate), Cfb—Temperate rainy with no dry season (oceanic climate), Cfc—Temperate rainy cold with no dry season (subpolar oceanic climate).

2.2. Data Processing

This study introduces a novel methodological approach for continental-scale pollution corridor analysis, combining comprehensive descriptive statistics with advanced visualization techniques. The analyses were performed using hourly data across 8 cities clustered into 4 groups according to their latitudinal similarities, representing the first systematic continental-scale pollution assessment in South America. To overcome limitations of commonly used 3D projections (contour plots) that oversimplify high pollution conditions through excessive

smoothing, we developed frequency of occurrence behaviour visualizations for PM_{10} and $PM_{2.5}$ that preserve critical extreme pollution events. With the raw data from each monitoring station (Figure 2a,b), frequency histograms of the PM_{10} and $PM_{2.5}$ concentrations (hourly registry) were calculated in classes spaced every 10 µg m^{-3} (Figure 2d,e). Previously, coarse PM concentrations were obtained by subtraction of $PM_{2.5}$ from PM_{10} (Figure 2c). Once the histograms were prepared, accumulative probabilities were calculated, showing the exceedance probabilities for concentration of particulate matter (Figure 2f,g). These probabilities were plotted in Figure 2h. The fine PM exceedance probability concentration was plotted on the abscissa axis, while the probability that coarse PM exceeded a certain concentration was plotted on the ordinate axis. In this way, the vertical and horizontal division lines represent percentiles, so that the fine PM and coarse PM concentrations equivalent to any probability can be determined from visual inspection.

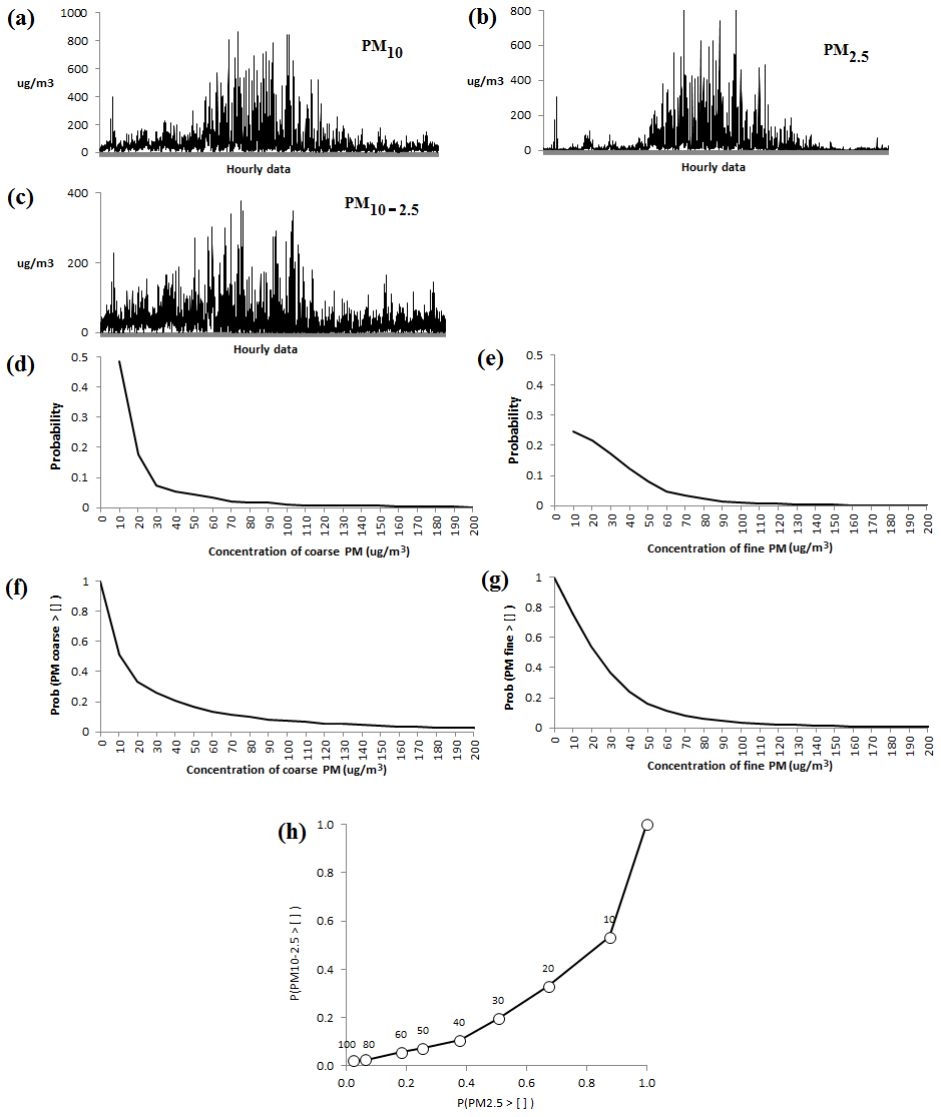


Figure 2. Data processing workflow for PM concentration analysis: (**a**) Raw hourly PM_{10} concentration data from monitoring stations. (**b**) Raw hourly $PM_{2.5}$ concentration data. (**c**) Calculated coarse PM concentrations obtained by subtracting $PM_{2.5}$ from PM_{10}. (**d**) Frequency histogram of $PM_{2.5}$ concentrations (hourly registry) in 10 µg m^{-3} bins. (**e**) Frequency histogram of PM_{10} concentrations. (**f**) Cumulative exceedance probability curve for $PM_{2.5}$. (**g**) Cumulative exceedance probability curve for coarse PM. (**h**) Bivariate probability plot showing fine PM exceedance probability (x-axis) versus coarse PM exceedance probability (y-axis), with division lines representing percentiles facilitating visual determination of PM concentrations at any probability level.

In Figure 2h, the shift of the curve to the right indicated that fine PM was more concerning than coarse PM. In contrast, the shift of the curve upwards indicated that fine PM was less concerning than coarse PM. The intercept of each curve with a 50% probability represented the median of the data. Using asymmetric distributions such as air pollution frequency histograms, the median should be considered more appropriate than the mean as a central tendency trait. In order to obtain an estimate of preponderance of fine PM over coarse PM, ratios can be calculated using the medians of the histograms.

Data quality control procedures followed standard environmental monitoring protocols: hourly measurements were screened for instrument malfunction flags, negative values were excluded, and data completeness thresholds required >75% valid hourly measurements per day for inclusion in daily statistics. Data files were processed using matrix-based routines written in Dev C++ 5.11 implementing standard statistical algorithms (frequency histograms with 10 $\mu g\,m^{-3}$ bins, cumulative probability calculations, and percentile extraction). Statistical correlations between RWC intensity indicators and PM concentrations were evaluated using linear regression analysis, with R^2 coefficients and *p*-values calculated to assess relationship strength and significance. Spreadsheet (MS-Excel) was used for the graphs. Bivariate polar graphs were created using the `polarPlot()` function in the R OPENAIR (v2.1-0) software package [52,53].

3. Results and Discussion

3.1. Description of Urban Air Quality Using Diurnal Averages

Table 2 presents the comprehensive statistics for PM_{10} and $PM_{2.5}$ concentrations across the unprecedented 1400 km pollution corridor spanning eight major urban centers from 1 January to 31 December for the years 2014 and 2015. This analysis establishes the first quantitative documentation of pollution patterns across the most extensive continuous urban air quality monitoring network in South America. The data demonstrate that annual mean PM_{10} concentrations systematically exceed the Chilean "chronic exposure" standard of 50 $\mu g\,m^{-3}$ across this entire continental-scale corridor. Kavouras et al. [31] for the year 1998 documented that PM_{10} concentrations for Rancagua and Temuco were 73.8 and 67.7 $\mu g\,m^{-3}$, respectively. Celis et al. [34] found a mean PM_{10} concentration of 86.2 $\mu g\,m^{-3}$ for Chillan during the period of 2001–2003. These comparisons demonstrate that the PM_{10} concentrations for the 2010 decade in the cities of southern Chile were lower than the past. Only in the city of Rancagua, the PM_{10} concentrations remained unchanged. The median of the data represented 50% of cumulative probability for the condition of the urban air. For Santiago and Rancagua, median of the PM_{10} concentration was over 70 $\mu g\,m^{-3}$. For the rest of the cities at higher latitudes, the median varied between 31–45 $\mu g\,m^{-3}$. The data establish a clear latitudinal decline in the mode value of PM_{10} concentrations as latitude increased. On the other hand, for all the cities, PM_{10} concentrations for the 98th percentile exceeded 150 $\mu g\,m^{-3}$, which is the "acute exposure" standard. Therefore, this parameter confirms that all cities are saturated by PM_{10}.

According to the Table 2, this annual mean surpassed the Chilean "chronic exposure" standard of $PM_{2.5}$ of 20 $\mu g\,m^{-3}$ in all the cities. This increased $PM_{2.5}$ is a new trend and was not reported early in the cities of Southern Chile. For Rancagua and Temuco, in 1998 the annual means for $PM_{2.5}$ were 42.6 and 35.2 $\mu g\,m^{-3}$, respectively [31]. Likewise, for the 98th percentile, all the studied cities exceeded the Chilean standard of 50 $\mu g\,m^{-3}$. However, the PM_{10} of these cities surpasses the Chilean standard much more extensively than the $PM_{2.5}$ and the situation worsened as latitude increased. The high range of $PM_{2.5}$ and PM_{10} in Santiago is due to being a metropolitan area, inhabited by more than 7 million people and, therefore, multiple predominant factors increase the PM level. At the same time, low

probabilities of the high concentration of PM may be explained by the implementation of decontamination plans.

Table 2. Statistics of daily PM data for the 8 cities under study (latitudinal order).

PM	Statistics	STG	RAN	TAL	CHI	LAN	TEM	OSO	COY
PM_{10}	Mean	70.6	76.3	59.1	52.2	56.9	50.6	50.9	64.8
	Median	62.1	68.8	45.3	38.7	45.4	36	31	44.5
	Mode	50–60	50–60	30–40	30–40	30–40	20–30	20–30	20–30
	98th percentile	160	168.2	180.7	174.9	180.3	174.9	223.6	214.9
	P (>195 µg m^{-3})	0.40%	0.50%	0.00%	1.20%	0.70%	1.20%	2.90%	3.30%
$PM_{2.5}$	Mean	30.6	26.5	31.8	32.2	30.4	33.7	34.3	52.1
	Median	25.9	17.5	16	16.3	16.3	18.3	18.3	32.1
	Mode	20–30	10–20	0–10	0–10	0–10	0–10	0–10	10–20
	98th percentile	78.7	87.8	134.5	150.7	134.5	144.8	181.4	186.7
	P (>80 µg m^{-3})	2.00%	3.80%	10.70%	10.30%	8.20%	11.40%	10.70%	22.60%
	P (>110 µg m^{-3})	0.10%	0.60%	4.80%	6.00%	3.80%	6.00%	6.70%	13.10%
	P (>170 µg m^{-3})	0.00%	0.00%	0.40%	1.10%	1.10%	1.20%	2.70%	3.30%

Osorno and Coyhaique showed high probability of environmental emergencies, as PM_{10} exceeded 195 µg m^{-3} ("alert level" in Chile) by around 3% during 11 days through the year. However, for $PM_{2.5}$ the probability of exceeding 80 µg m^{-3} ("alert level") was above 2% (7 days) for all the cities. While for Santiago this probability was 2%, for Rancagua it increased up to 3.8%. However, most importantly, in both cities "pre–emergency level" (exceeding 110 µg m^{-3}) was rare and "emergency level" (exceeding 170 µg m^{-3}) was non-existent. For the five remaining cities located in the central valley (Talca, Chillan, Los Angeles, Temuco and Osorno), the probability of exceeding the alert level was greater than 5% and the pre-emergency level was double. The emergency levels were under 1.2% for the first four cities, except for Osorno (2.7%). For the Patagonian city of Coyhaique, critical air quality emergencies occur with alarming frequency as demonstrated in Table 2. The Global Urban Ambient Air Pollution Database [54], which compiled mean annual data from 2014 for 2613 cities worldwide, establishes Coyhaique as ranking among the world's most severely polluted cities, placing in the 95th percentile globally for $PM_{2.5}$ concentrations—a finding that positions this Patagonian city among the most extreme pollution hotspots on Earth. The other Chilean cities in this study rank between the 75th and 85th percentiles globally, indicating that Chile's entire central-southern corridor represents an international pollution crisis of unprecedented scale. This global ranking becomes even more significant considering that many cities in developing countries lack comprehensive air quality monitoring systems [55], suggesting that documented pollution levels represent only the measurable portion of a worldwide crisis. Recent global air quality assessments [56] and WHO database updates [57] continue to demonstrate the severity of PM pollution worldwide, with the Global Burden of Disease studies [58] quantifying major air pollution sources and their health impacts.

3.2. Variability of Fine and Coarse PM by City

Figure 3a shows probabilities of fine PM and coarse PM over a certain concentration during three periods of the year for Santiago: from January to April is shown in circles, May to August is shown in squares (cold season), and September to December is shown in triangles. Since the data were not smoothed in the construction of these diagrams, the conditions with poor air quality are highlighted. For $PM_{2.5}$, the median ranged from 23 µg m^{-3} in the first third of the year to 40 µg m^{-3} during the cold season and dropped to 19 µg m^{-3} during the last part of the year. For PM_{10}, the median reached 38, 38, and

30 µg m^{-3} for every third of the year. During the cold season, 80% of the time the concentration of $PM_{2.5}$ exceeded 20 µg m^{-3}, which was the saturation threshold for the annual mean of $PM_{2.5}$. During the first and last third of the year, the mode of $PM_{2.5}$ was in the range of 10–30 µg m^{-3}. In these seasons, the histograms were highly asymmetrical are displaced towards low PM concentrations. On the contrary, for the colder season the histogram was flat, which probed by more constant spacing between the points within the same curve. Figure 3b shows probabilities of fine PM and coarse PM over a certain concentration during three periods of the day for Santiago during the cold season. These hours were chosen as they corresponded to extreme situations: at 22:00 (triangles) the pollution reached a peak and at 15:00 (squares) it occurred at a minimum. The time of 07:00 (circles) was chosen for having an equidistant curve from the others. The displacement of the curves shows that the fine MP tends to show an increase during the afternoon, followed by evenings, and then decreases during the morning hours. Figure 3c,d shows bivariate polar plots of mean fine PM and coarse PM concentrations given wind speed and direction for Santiago. Graphs indicate that fine PM and coarse PM originate from the W, SW, and SE directions. Source apportionment for Santiago indicated that 28.9% of $PM_{2.5}$ [59] came from wood burning outside Santiago from the population located in the south-west of the metropolitan region [60]. A total of 9.7% came from three copper foundries located 100 km NW (Ventanas), 70 km N (Chagres), and 60 km SE (Caletones). At a distance of 90 km to the west we find the Pacific Ocean, which contributed to 9.9% of $PM_{2.5}$ from marine aerosols. An amount of 16.2% were sulfates mainly originating from gas-to-particle conversion from SO_2, [61]. Jorquera and Barraza [59] indicated that 3.9% of $PM_{2.5}$ came from soil dust, but alternatively [42] indicated that above 50% of PM_{10} pollution were soil particles. With 45–58% of the coarse PM corresponding to fine PM (Figure 3a,b), these data conclusively demonstrate that the majority of coarse PM originates from soil particles, representing a statistically significant deviation from typical urban pollution source profiles.

For Rancagua, the values for seasonal medians of $PM_{2.5}$ were very similar to those of Santiago (Figure 4a). These varied from 20 µg m^{-3} in the first third of the year, increased to 42 µg m^{-3} during the cold season, and were reduced to 17 µg m^{-3} during the last third of the year. The same as in Santiago, during the cold season 80% of the time the $PM_{2.5}$ concentration exceeded 20 µg m^{-3}. Histograms for $PM_{2.5}$ during the cold season were found to be very similar between the two cities even though the population of Santiago is approximately 30 times higher than Rancagua. For PM_{10}, median values were found to be higher than Santiago, reaching 45, 35, and 35 µg m^{-3} in each third of the year, respectively. The value of the first four months of the year was especially noteworthy, because in no other southern city did the median exceed 20 µg m^{-3} in any season of the year. Figure 4b shows that the fine PM tends to increase strongly at night and to decrease passing midday. For Rancagua, Figure 4c,d shows that for low wind speeds, $PM_{2.5}$ reached high concentrations, which are frequently expected at urban sites with higher $PM_{2.5}$ concentrations result from largely stable atmospheric conditions and also reduced advection. Both fine PM and coarse PM showed directions SW and ENE. The PM arrived mainly from the SW, which coincides with the prominent wind direction but a source was marked at 70° (ENE) from the monitoring station in the direction of the Caletones copper foundry 25 km which could be a possible cause for the particulate matter. This was confirmed by using the conditional bivariate probability function approach from Carslaw and Ropkins [52] (graphs not showed). This hypothesis had previously been suggested by Koutrakis et al. [41] but no evidence was provided to support this.

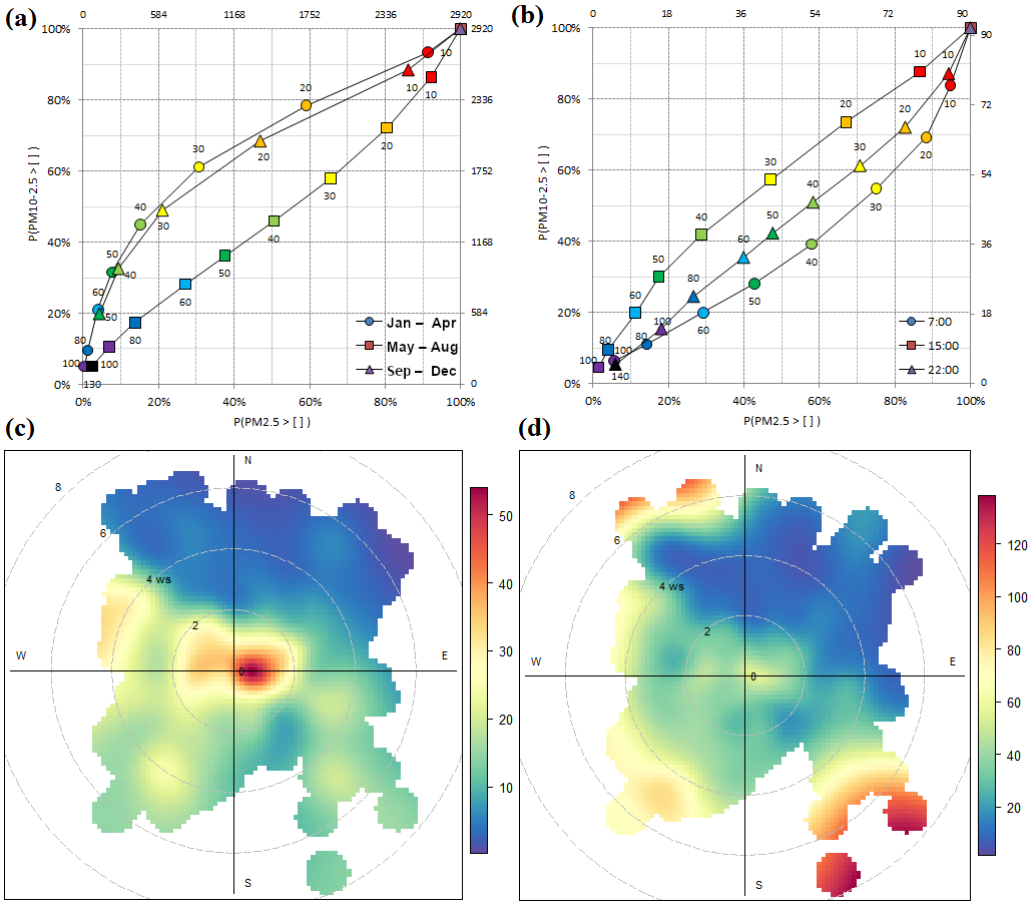


Figure 3. (**a**) Probability curves of fine PM and coarse PM concentrations for Santiago per periods of three months each. (**b**) Probability curves of fine PM and coarse concentrations in three different periods of the day during the cold season. The values within the graphs indicate the concentrations in μg m^{-3}. For each graph, secondary axes indicate the number of hours at which the concentrations exceeded. (**c**) Bivariate polar plot for mean concentration of $PM_{2.5}$ by wind speed and direction. (**d**) Bivariate polar plot for mean concentration of coarse PM by wind speed and direction. For each polar plot, the radius was an indicator of wind speed (m s^{-1}) while the color showed the mean PM concentration.

Figure 5 showing the condition for Talca will be used to represent the cluster of 5 cities: Talca, Los Angeles, Chillan, Temuco, and Osorno. During the cold season, 70% of the time the $PM_{2.5}$ concentration exceeded 20 μg m^{-3}. Moreover, for PM_{10}, the median values reached 28, 18, and 18 μg m^{-3} on each third of the year. The mode for $PM_{2.5}$ was 0–10 μg m^{-3} in the first and last third of the year and increased to 10–20 μg m^{-3} during the cold season. All these indicators, when compared to Rancagua, show that air quality for PM in Talca was relatively better. Both cities have a similar population (around 220,000 inhabitants) and industrialization level. Both cities also have the same climatic pattern because of the relative position between two mountain ranges. In order to understand the differences, a more detailed analysis was conducted using the information provided by Figures 4 and 5. For the Talca–Los Angeles–Chillan–Temuco cluster, during the first third-of-year the ratio of fine PM to coarse PM was around 30% and increased to 68% during the cold season, falling again to 31% in the last third of the year. This winter-associated increase in the ratio of fine PM over coarse PM became more pronounced as latitude increased. The rise in ratio during the cold season conclusively establishes the dominant role of residential wood combustion (RWC) as the primary source of PM throughout the region. The particles emitted by the combustion of firewood in stoves and

small residential heaters had a concentrated size distribution between 0.15 and 0.4 µm. For small stoves, between 80–95% of PM_{10} emitted was found to be $PM_{2.5}$ [61,62], but in larger combustion systems this ratio did not exceed 90% [63,64]. The peak concentration of $PM_{2.5}$, as seen in Figure 5c, overlaps with low wind speed, conclusively establishing the local origin of $PM_{2.5}$. The conditional bivariate probability function approach established that at low $PM_{2.5}$ concentrations particulate originated from almost all directions. However, for high $PM_{2.5}$ concentrations, the particles were from local origin and related to very low wind speed. On the contrary, coarse PM came from sources other than the representative area of the monitoring station matching with prominent wind direction in the warm season (Figure 5d). As such, it has been reported that fugitive dust (geological material) from agriculture, erosion, and roads were the major contributors to PM_{10} at nearly all sampling sites worldwide, often contributing up to 50% of the mean PM_{10} concentration [64].

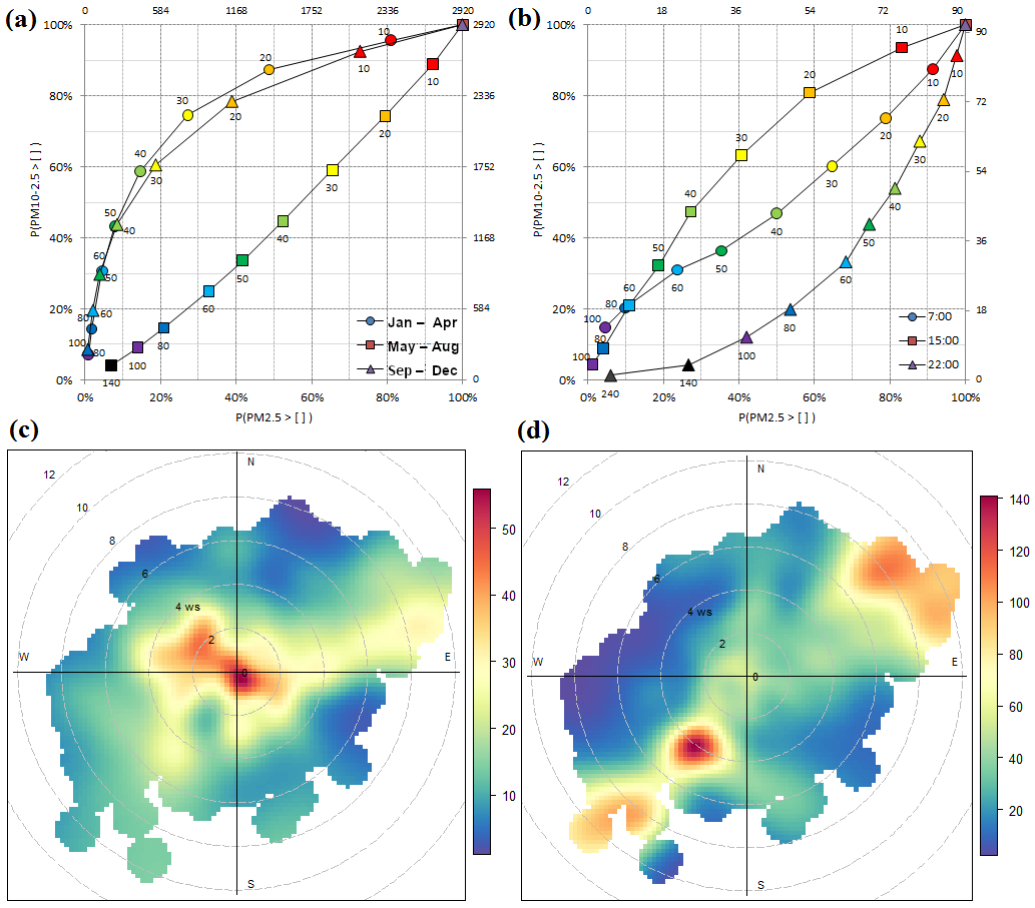


Figure 4. (**a**) Probability curves of fine PM and coarse PM concentrations for Rancagua per periods of three months each. (**b**) Probability curves of fine PM and coarse concentrations in three different periods of the day during the cold season. The values within the graphs indicate the concentrations in µg m^{-3}. For each graph, secondary axes indicate the number of hours at which the concentrations exceeded. (**c**) Bivariate polar plot for mean concentration of $PM_{2.5}$ by wind speed and direction. (**d**) Bivariate polar plot for mean concentration of coarse PM by wind speed and direction. For each polar plot, the radius was an indicator of wind speed (m s^{-1}) while the color showed the mean PM concentration.

For Coyhaique (Figure 6) the median values for fine PM varied from 15 µg m^{-3} in the first third of the year, increasing strongly to 75 µg m^{-3} during the cold season and reducing to 21 µg m^{-3} during the last third-of-year. The mode for $PM_{2.5}$ was 0–10 µg m^{-3} in first third-of-year increased to 30–40 µg m^{-3} during the cold season and reduced to 10–20 µg m^{-3} in last third-of-year. During the cold season, almost 90% of the time

the $PM_{2.5}$ concentration exceeded the Chilean standard. For coarse PM, the median values remained low throughout the year, reaching 9, 12, and 10 µg m^{-3} on each third-of-year. During the first third-of-year, the ratio of $PM_{2.5}$ to PM_{10} was around 63% and reached an extraordinary 86% during the cold season, falling again to 64% in the last third-of-year. This 86% fine particulate matter ratio represents one of the most extreme values documented globally, far exceeding typical urban fine PM ratios of 50–70% reported in major international pollution studies, establishing Coyhaique as an unprecedented case study in fine particulate matter dominance. Figure 6b reveals that median concentrations throughout the day for $PM_{2.5}$ reached 90, 49, and 120 µg m^{-3} at 07:00, 15:00, and 22:00, respectively; whereas coarse PM medians remained remarkably constant around 12 µg m^{-3} throughout the entire day. Consequently, diurnal variations of this ratio during the cold season were calculated as 88%, 80%, and 90% at 07:00, 15:00, and 22:00, respectively. This exceptionally minimal variation demonstrates the continuous, intensive use of RWC throughout the entire day [65], representing a consistent pollution pattern in scientific literature.

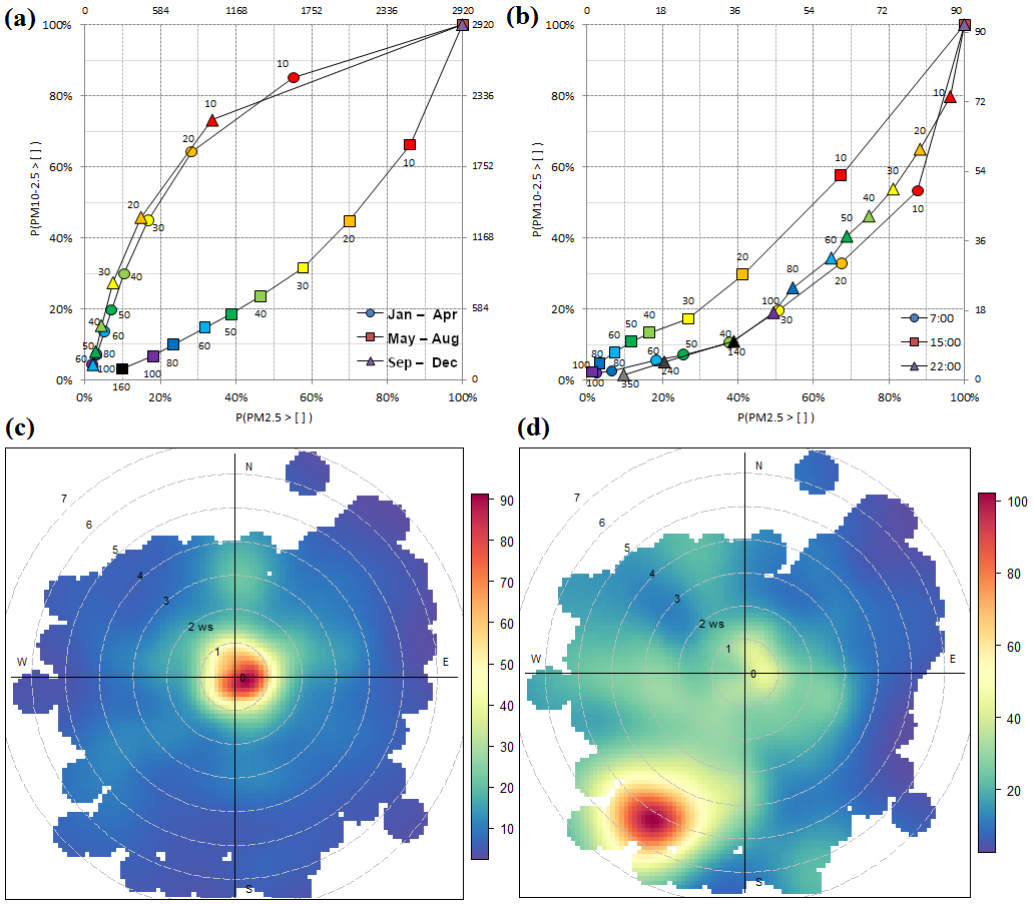


Figure 5. (**a**) Probability curves of $PM_{2.5}$ and PM_{10} concentrations for Talca (clustering Talca, Los Angeles, Chillan, Temuco, and Osorno) per periods of three months each. (**b**) Probability curves of fine PM and coarse concentrations in three different periods of the day during the cold season. The values within the graphs indicate the concentrations in µg m^{-3}. For each graph, secondary axes indicate the number of hours at which the concentrations exceeded. (**c**) Bivariate polar plot for mean concentration of $PM_{2.5}$ by wind speed and direction. (**d**) Bivariate polar plot for mean concentration of coarse PM by wind speed and direction. For each polar plot, the radius was an indicator of wind speed (m s^{-1}) while the color showed the mean PM concentration.

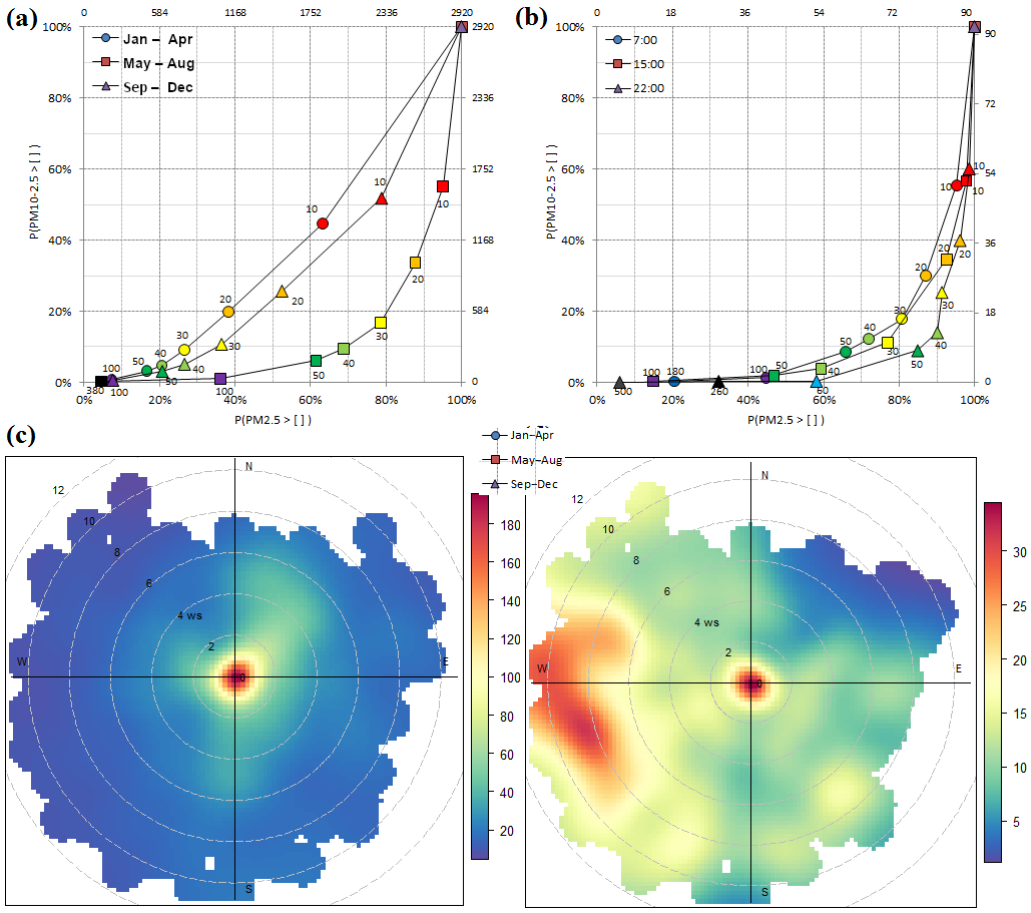


Figure 6. (**a**) Probability curves of fine PM and coarse PM concentrations for Coyhaique per periods of three months each. (**b**) Probability curves of fine PM and coarse concentrations in three different periods of the day during the cold season. The values within the graphs indicate the concentrations in μg m^{-3}. For each graph, secondary axes indicate the number of hours at which the concentrations exceeded. (**c**) Bivariate polar plot for mean concentration of $PM_{2.5}$ by wind speed and direction. (**d**) Bivariate polar plot for mean concentration of coarse PM by wind speed and direction. For each polar plot, the radius was an indicator of wind speed (m s^{-1}) while the color showed the mean PM concentration.

3.3. Relationship Between Urban Air Quality and Intensity of Firewood Use

Ministerio de Energía [11] compiled the quantity of different types of stoves used for RWC in the study area. The results indicate that intensity of RWC use increases with latitude. In fact, it has been determined that above latitude 38° S (Temuco), more than 80% and almost 100% of households in consume firewood in urban and rural areas, respectively [44]. SICAM-Ingeniería [66] compiled the emission factors for fine PM for different stoves technologies. Using statistical data of population and size of cities, we estimated intensity of firewood use parameters such as stoves/hectare, stoves/household and inventories of PM emission. Table 3 presents the outcome of the regression analysis of the concentration of fine and coarse PM in the cold season (May–August) compared with the rate of firewood consumption, the spatial frequency of stoves, the mean of stoves per household and inventory of PM or cumulated PM emissions per year. All the correlations for $PM_{2.5}$ in this study demonstrated significant or highly significant relationships. In the case of coarse PM there was no correlation with indicators of intensity of firewood use.

Table 3. R^2 correlating intensity of RWC use and PM concentration during cold season.

Independent Variable	Mean Fine PM	Mean Coarse PM
Firewood consumption	0.965 **	0.3
Stoves/hectare	0.887 *	0.008
Stoves/household	0.824 *	0.005
Inventory of PM/hectare	0.966 **	0.001
Inventory of PM/household	0.946 **	0

* p-value ≤ 0.05; ** p-value ≤ 0.01.

4. Conclusions

This study presents a latitudinal analysis of $PM_{2.5}$ and PM_{10} across a 1400 km pollution corridor spanning Chile's central-southern zone. The analysis reveals significant pollution gradients, with Coyhaique ranking one the most polluted cities worldwide (95th percentile globally) and demonstrating an 86% fine particulate matter ratio that exceeds typical international urban standards [54,67].

The described pollution patterns represent a significant continental-scale environmental concern, with 4900–6500 annual premature deaths directly attributable to $PM_{2.5}$ exposure across the study corridor [12,13]. The systematic correlation between RWC intensity and fine PM concentrations ($R^2 > 0.96$) suggest that RWC as the dominant pollution driver across multiple climate zones and topographical settings.

Our findings provide a methodological framework applicable to mountain-valley pollution systems globally while establishing pre-Paris Agreement baseline data for evaluating climate mitigation strategies [14,15,25,45].

The evidence supports implementation of comprehensive wood combustion control strategies across Chile's central-southern corridor. Practical policy interventions should prioritize: (1) subsidized replacement programs transitioning households from traditional wood stoves to cleaner heating technologies such as pellet stoves, heat pumps, or natural gas systems; (2) establishing regulatory standards for wood moisture content and combustion efficiency to reduce emissions from existing stoves; and (3) developing financial incentives and technical assistance programs that address affordability barriers for urban households where heating infrastructure transitions require substantial investment. International experience from European biomass heating regions demonstrates that combining economic subsidies with public awareness campaigns and strict emission standards can achieve significant air quality improvements [38]. This research provides essential baseline documentation for national air quality policy and international climate change assessment frameworks. The temporal context provides valuable pre-intervention baselines for evaluating subsequent policy effectiveness and climate-related changes in pollution patterns.

Future research should consider these baselines to quantify intervention effectiveness and regional pollution evolution under changing climatic conditions. The methodological framework developed here provides a replicable approach for longitudinal monitoring of pollution corridors worldwide, particularly in mountain-valley systems experiencing environmental change.

Study Limitations: This analysis is constrained by several factors that should inform interpretation of results. First, the 2014–2015 temporal scope represents a snapshot baseline and cannot capture long-term trends or recent changes in heating practices and emission control policies. Second, while the SINCA monitoring network provides unprecedented South American coverage, station placement within cities may not fully represent exposure gradients across diverse urban microenvironments. Third, the correlation analysis establishes strong statistical relationships between RWC indicators and PM concentrations but

does not quantify contributions from other potential sources (vehicle emissions, industrial activities, long-range transport). Finally, meteorological variables beyond wind speed and direction—particularly mixing layer height dynamics and precipitation patterns—warrant more comprehensive integration into future source apportionment analyses.

Author Contributions: Conceptualization, R.B.; methodology, R.B.; software, R.B. and B.I.; validation, R.B. and B.I.; formal analysis, R.B.; investigation, R.B. and B.I.; resources, R.B. and B.I.; data curation, R.B. and B.I.; writing—original draft preparation, R.B. and B.I.; writing—review and editing, R.B. and B.I.; visualization, R.B. and B.I.; supervision, R.B.; project administration, R.B.; funding acquisition, R.B. All authors have read and agreed to the published version of the manuscript.

Funding: This research received no external funding.

Data Availability Statement: The data used in this study was downloaded in ASCII format from the SINCA network belonging to the Chilean Ministry of the Environment http://sinca.mma.gob.cl/, accessed on 1 August 2025.

Conflicts of Interest: The authors declare no conflicts of interest.

Abbreviations

The following abbreviations are used in this manuscript:

PM	Particulate Matter
RWC	Residential wood combustion
WHO	World Health Organisation
RETC	Registro de Emisiones y Transferencia de Contaminantes (Pollutant emission and transfer register)
MASL	Meters above sea level

References

1. Schwartz, J.; Dockery, D.; Neas, L. Is daily mortality associated specifically with fine particles? *J. Air Waste Manag. Assoc.* **1996**, *46*, 927–939. [CrossRef]
2. Raaschou-Nielsen, O.; Sørensen, M.; Ketzel, M.; Hertel, O.; Loft, S.; Tjønneland, A.; Overvad, K.; Andersen, Z. Long-term exposure to traffic-related air pollution and diabetes-associated mortality: A cohort study. *Diabetologia* **2013**, *56*, 36–46. [CrossRef]
3. Franchini, M.; Mannucci, P. Mitigation of air pollution by greenness: A narrative review. *Eur. J. Intern. Med.* **2018**, *55*, 1–5. [CrossRef]
4. Vowles, M.; Kerry, R.; Ingram, B.; Mason, B. Investigation of the environmental and socio-economic characteristics of counties with a high asthma burden to focus asthma action in Utah. *Int. J. Environ. Res. Public Health* **2020**, *17*, 5251. [CrossRef]
5. Lee, L.Y.; Kerry, R.; Ingram, B.; Golden, C.S.; LeMonte, J.J. Investigating the Spatial Patterns of Heavy Metals in Topsoil and Asthma in the Western Salt Lake Valley, Utah. *Environments* **2024**, *11*, 223. [CrossRef]
6. Straif, K.; Cohen, A.; Samet, J.; International Agency for Research on Cancer. *Air Pollution and Cancer*; IARC Scientific Publication No. 161; IARC Scientific: Lyon, France, 2013.
7. Ministerio del Medio Ambiente. *Informe del Estado del Medio Ambiente, Capítulo 1; Contaminación del Aire*; Technical Report; Ministerio del Medio Ambiente: Santiago, Chile, 2012.
8. Ministerio de Desarrollo Social. *Estimación del Valor de la Vida Estadística en Chile a Través del Enfoque de Disposición a Pagar*; Technical Report. Ministerio de Desarrollo Social, División de Evaluación Social de Inversiones. Ministerio de Desarrollo Social: Santiago, Chile, 2018.
9. Ministerio Secretaría General de la Presidencia. Decreto Supremo N° 59. Establece Norma de Calidad Primaria para Material Particulado Respirable MP10, en Especial de los Valores que Definen Situaciones de Emergencia. Technical Report. 2018. Available online: https://www.bcn.cl/leychile/navegar?idNorma=99434 (accessed on 12 April 2018).
10. Ministerio del Medio Ambiente. Decreto Supremo N° 12. Establece Norma Primaria de Calidad Ambiental para Material Particulado Fino Respirable MP2.5. Technical Report. 2018. Available online: https://www.bcn.cl/leychile/Navegar?idNorma=1025202 (accessed on 14 May 2018).
11. Ministerio de Energía. *Política de Uso de la Leña y Sus Derivados para Calefacción*; Technical Report; División de Eficiencia Energética, Ministerio de Energía: Santiago, Chile 2016. Available online: https://www.minenergia.cl/archivos_bajar/2016/03/politica_lena_2016_web.pdf (accessed on 14 May 2018).

12. HEI International. State of Global Air 2017: A Special Report on Global Exposure to Air Pollution and Its Disease Burden. 2018. Available online: https://www.ccacoalition.org/resources/state-global-air-2017-special-report-global-exposure-air-pollution-and-its-disease-burden (accessed on 4 April 2018).
13. World Health Organization. A Global Campaign for Clean Air. Discover How the Air in Your City Impacts You. 2018. Available online: https://www.ccacoalition.org/resources/breathelife-global-campaign-clean-air (accessed on 14 May 2018).
14. Peláez, L.M.G.; Santos, J.M.; de Almeida Albuquerque, T.T.; Reis, N.C., Jr.; Andreão, W.L.; de Fátima Andrade, M. Air quality status and trends over large cities in South America. *Environ. Sci. Policy* **2020**, *114*, 422–435. [CrossRef]
15. Molina, L.T.; Gallardo, L.; Andrade, M.; Baumgardner, D.; Borbor-Córdova, M.; Bórquez, R.; Casassa, G.; Cereceda-Balic, F.; Dawidowski, L.; Garreaud, R.; et al. Pollution and its Impacts on the South American Cryosphere. *Earth's Future* **2015**, *3*, 345–369. [CrossRef]
16. Andreae, M.; Andreae, T.; Annegarn, H.; Beer, J.; Cachier, H.; Le Canut, P.; Elbert, W.; Maenhaut, W.; Salma, I.; Wienhold, F.; et al. Airborne studies of aerosol emissions from savanna fires in southern Africa: 2. Aerosol chemical composition. *J. Geophys. Res. Atmos.* **1998**, *103*, 32119–32128. [CrossRef]
17. Samsonov, Y.; Ivanov, V.; McRae, D.; Baker, S. Chemical and dispersal characteristics of particulate emissions from forest fires in Siberia. *Int. J. Wildland Fire* **2012**, *21*, 818–827. [CrossRef]
18. Sarigiannis, D.; Karakitsios, S.; Kermenidou, M.; Nikolaki, S.; Zikopoulos, D.; Semelidis, S.; Papagiannakis, P.; Tzimou, R. Total exposure to airborne particulate matter in cities: The effect of biomass combustion. *Sci. Total Environ.* **2014**, *493*, 795–805. [CrossRef]
19. Ponce-Donoso, M.; Vallejos-Barra, O.; Ingram, B.; Daniluk-Mosquera, G. Urban trees and environmental variables: Relationships in a city of central Chile. *Arboric. Urban For.* **2020**, *45*, 84–95. [CrossRef]
20. Rutllant, J.; Garreaud, R. Meteorological Air Pollution Potential for Santiago, Chile: Towards an Objective Episode Forecasting. *Environ. Monit. Assess.* **1995**, *34*, 223–244. [CrossRef]
21. Escribano, J.; Gallardo, L.; Rondanelli, R.; Choi, Y. Satellite retrievals of aerosol optical depth over a subtropical urban area: The role of stratification and surface reflectance. *Aerosol Air Qual. Res.* **2014**, *14*, 596–607. [CrossRef]
22. Gramsch, E.; Catalán, L.; Ormeño, I.; Palma, G. Traffic and seasonal dependence of the light absorption coefficient in Santiago de Chile. *Appl. Opt.* **2000**, *39*, 4895–4901. [CrossRef] [PubMed]
23. Gramsch, E.; Cáceres, D.; Oyola, P.; Reyes, F.; Vásquez, Y.; Rubio, M.; Sánchez, G. Influence of surface and subsidence thermal inversion on $PM_{2.5}$ and black carbon concentration. *Atmos. Environ.* **2014**, *98*, 290–298. [CrossRef]
24. Salini, G. Desarrollo de un Modelo para Pronosticar Concentraciones de PM2.5 en Santiago. Ph.D. Thesis, Facultad de Ciencias Departamento de Física, Universidad de Santiago de Chile, Santiago, Chile, 2009.
25. De Wekker, S.F.J.; Kossmann, M. Convective Boundary Layer Heights Over Mountainous Terrain—A Review of Concepts. *Front. Earth Sci.* **2015**, *3*, 77. [CrossRef]
26. Solanki, R.; Macatangay, R.; Sakulsupich, V.; Sonkaew, T.; Mahapatra, P.S. Mixing Layer Height Retrievals From MiniMPL Measurements in the Chiang Mai Valley: Implications for Particulate Matter Pollution. *Front. Earth Sci.* **2019**, *7*, 308. [CrossRef]
27. Herrera-Mejía, L.; Hoyos, C.D. Characterization of the atmospheric boundary layer in a narrow tropical valley using remote-sensing and radiosonde observations and the WRF model: The Aburrá Valley case-study. *Q. J. R. Meteorol. Soc.* **2019**, *145*, 2641–2665. [CrossRef]
28. Pierce, A.M.; Loría-Salazar, S.M.; Holmes, H.A.; Gustin, M.S. Investigating horizontal and vertical pollution gradients in the atmosphere associated with an urban location in complex terrain, Reno, Nevada, USA. *Atmos. Environ.* **2019**, *196*, 103–117. [CrossRef]
29. Hallar, A.G.; Brown, S.S.; Crosman, E.; Barsanti, K.C.; Cappa, C.D.; Faloona, I.; Fast, J.; Holmes, H.A.; Horel, J.; Lin, J.; et al. Coupled Air Quality and Boundary-Layer Meteorology in Western U.S. Basins during Winter: Design and Rationale for a Comprehensive Study. *Bull. Am. Meteorol. Soc.* **2021**, *102*, E2012–E2033. [CrossRef]
30. Zhang, H.; Huang, W.; Shen, X.; Ramisetty, R.; Song, J.; Kiseleva, O.; Holst, C.C.; Khan, B.; Leisner, T.; Saathoff, H. Aerosol composition, air quality, and boundary layer dynamics in the urban background of Stuttgart in winter. *Atmos. Chem. Phys.* **2024**, *24*, 10617–10637. [CrossRef]
31. Kavouras, I.; Koutrakis, P.; Cereceda-Balic, F.; Oyola, P. Source apportionment of PM_{10} and PM_{25} in five Chilean cities using factor analysis. *J. Air Waste Manag. Assoc.* **2001**, *51*, 451–464. [CrossRef]
32. Tsapakis, M.; Lagoudaki, E.; Stephanou, E.; Kavouras, I.; Koutrakis, P.; Oyola, P.; Von Baer, D. The composition and sources of $PM_{2.5}$ organic aerosol in two urban areas of Chile. *Atmos. Environ.* **2002**, *36*, 3851–3863. [CrossRef]
33. Carvacho, O.; Trzepla-Nabaglo, K.; Ashbaugh, L.; Flocchini, R.; Melín, P.; Celis, J. Elemental composition of springtime aerosol in Chillán, Chile. *Atmos. Environ.* **2004**, *38*, 5349–5352. [CrossRef]
34. Celis, J.E.; Morales, J.R.; Zaror, C.A.; Inzunza, J.C. A study of the particulate matter PM_{10} composition in the atmosphere of Chillán, Chile. *Chemosphere* **2004**, *54*, 541–550. [CrossRef] [PubMed]

35. Hedberg, E.; Gidhagen, L.; Johansson, C. Source contributions to PM10 and arsenic concentrations in Central Chile using positive matrix factorization. *Atmos. Environ.* **2005**, *39*, 549–561. [CrossRef]
36. Díaz-Robles, L.; Saavedra, H.; Schiappacasse, L.; Cereceda-Balic, F.; Cereceda, F.; Santa, T. The Air Quality in Chile. In *EM: Air and Waste Management Association's Magazine for Environmental Managers (2011)*; Air and Waste Management Association: Pittsburgh, PA, USA, 2011, pp. 28–33.
37. Pope, C.A., III; Muhlestein, J.B.; Anderson, J.L.; Cannon, J.B.; Hales, N.M.; Meredith, K.G.; Le, V.; Horne, B.D. Short-term exposure to fine particulate matter air pollution is preferentially associated with the risk of ST-segment elevation acute coronary events. *J. Am. Heart Assoc.* **2015**, *4*, e002506. [CrossRef]
38. Vardoulakis, S.; Johnston, F.; Goodman, N.; Morgan, G.; Jones, P.; Borchers Arriagada, N.; Smurthwaite, K.; Indu, G.; Robinson, D. Reducing exposure to residential wood smoke in Australia: Health equity, environmental justice, and implementation challenges and opportunities. In *Proceedings of the ISEE Conference Abstracts*; EHP Publishing: Research Triangle Park, NC, USA, 2024; Volume 2024.
39. Savolahti, M.; Karvosenoja, N.; Soimakallio, S.; Kupiainen, K.; Tissari, J.; Paunu, V.V. Near-term climate impacts of Finnish residential wood combustion. *Energy Policy* **2019**, *133*, 110837. [CrossRef]
40. Wu, D.; Zheng, H.; Li, Q.; Jin, L.; Lyu, R.; Ding, X.; Huo, Y.; Zhao, B.; Jiang, J.; Chen, J.; et al. Toxic potency-adjusted control of air pollution for solid fuel combustion. *Nat. Energy* **2022**, *7*, 194–202. [CrossRef]
41. Koutrakis, P.; Sax, S.; Sarnat, J.; Coull, B.; Demokritou, P.; Demokritou, P.; Oyola, P.; Garcia, J.; Gramsch, E. Analysis of PM_{10}, $PM_{2.5}$, and $PM_{2.5–10}$ Concentrations in Santiago, Chile, from 1989 to 2001. *J. Air Waste Manag. Assoc.* **2005**, *55*, 342–351. [CrossRef]
42. O'Ryan, R.; Larraguibel, L. Contaminación del aire en Santiago: ¿Qué es, qué se ha hecho, qué falta? *Rev. Perspect.* **2000**, *4*, 153–191.
43. Universidad de Chile. *Informe País: Estado del Medio Ambiente en Chile, 2008*. Technical Report; Centro de Análisis de Políticas Públicas, Universidad de Chile: Santiago, Chile, 2010.
44. Universidad de Chile. *Informe País: Estado del Medio Ambiente en Chile, 2005*; Technical Report; Centro de Análisis de Políticas Públicas, Universidad de Chile: Santiago, Chile, 2006.
45. Hamilton, I.; Kennard, H.; McGushin, A.; Höft, L.; Ebi, K.; Kelman, I.; Hess, J.; Haines, A. The public health implications of the Paris Agreement: A modelling study. *Lancet Planet. Health* **2021**, *5*, e74–e83. [CrossRef] [PubMed]
46. Real, E.; Couvidat, F.; Ung, A.; Malherbe, L.; Raux, B.; Gressent, A.; Colette, A. Historical reconstruction of background air pollution over France for 2000–2015. *Earth Syst. Sci. Data* **2022**, *14*, 2419–2443. [CrossRef]
47. Turnock, S.T.; Allen, R.J.; Andrews, M.; Bauer, S.E.; Deushi, M.; Emmons, L.; Good, P.; Horowitz, L.; John, J.G.; Michou, M.; et al. Historical and future changes in air pollutants from CMIP6 models. *Atmos. Chem. Phys.* **2020**, *20*, 14547–14579. [CrossRef]
48. Thomas, N.; Collow, A.; Bosilovich, M.; Dezfuli, A. Effect of baseline period on quantification of climate extremes over the United States. *Geophys. Res. Lett.* **2023**, *50*, e2023GL105204. [CrossRef]
49. Chen, C.f.; de Rubens, G.Z.; Xu, X.; Li, J. Coronavirus comes home? Energy use, home energy management, and the social-psychological factors of COVID-19. *Energy Res. Soc. Sci.* **2020**, *68*, 101688. [CrossRef]
50. Sangüesa, C.; Ibañez, A.; Pizarro, R.; Vidal-Silva, C.; García-Chevesich, P.; Mendoza, R.; Toledo, C.; Pino, J.; Paredes, R.; Ingram, B. A Sub-Hourly Precipitation Dataset from a Pluviographic Network in Central Chile. *Data* **2025**, *10*, 95. [CrossRef]
51. Pizarro-Tapia, R.; González-Leiva, F.; Valdes-Pineda, R.; Ingram, B.; Sangüesa, C.; Vallejos, C. A Rainfall Intensity Data Rescue Initiative for Central Chile Utilizing a Pluviograph Strip Charts Reader (PSCR). *Water* **2020**, *12*, 1887. [CrossRef]
52. Carslaw, D.C.; Ropkins, K. Openair—An R package for air quality data analysis. *Environ. Model. Softw.* **2012**, *27–28*, 52–61. [CrossRef]
53. R Development Core Team. *R: A Language and Environment for Statistical Computing*; R Foundation for Statistical Computing: Vienna, Austria, 2011; ISBN 3-900051-07-0.
54. World Health Organization. *Global Urban Ambient Air Pollution Database*; World Health Organization: Geneva, Switzerland, 2018.
55. Schwela, D.H.; Haq, G. Strengths and Weaknesses of the WHO Global Ambient Air Quality Database. *Aerosol Air Qual. Res.* **2020**, *20*, 1026–1037. [CrossRef]
56. IQAir. *2024 World Air Quality Report*; Technical Report; IQAir: Steinach, Switzerland, 2024.
57. World Health Organization. *WHO Ambient Air Quality Database*; World Health Organization: Geneva, Switzerland, 2024.
58. Global Burden of Disease from Major Air Pollution Sources (GBD MAPS): A Global Approach. Research Report. 2022. Available online: https://pmc.ncbi.nlm.nih.gov/articles/PMC9501767/ (accessed on 1 January 2018).
59. Jorquera, H.; Barraza, F. Source apportionment of ambient $PM_{2.5}$ in Santiago, Chile: 1999 and 2004 results. *Sci. Total Environ.* **2012**, *435*, 418–429. [CrossRef] [PubMed]
60. Valdivia, S.A.P. Análisis Temporal y Espacial de la Calidad del Aire Determinado por Material Particulado PM_{10} y $PM_{2,5}$ en Lima Metropolitana; Technical Report 2. 2016. Available online: https://revistas.lamolina.edu.pe/index.php/acu/article/view/699/pdf_37 (accessed on 1 January 2018).

61. Artaxo, P.; Oyola, P.; Martinez, R. Aerosol composition and source apportionment in Santiago de Chile. *Nucl. Instrum. Methods Phys. Res. Sect. B Beam Interact. Mater. Atoms* **1999**, *150*, 409–416. [CrossRef]
62. Kleeman, M.; Schauer, J.; Cass, G. Size and composition distribution of fine particulate matter emitted from wood burning, meat charbroiling, and cigarettes. *Environ. Sci. Technol.* **1999**, *33*, 3516–3523. [CrossRef]
63. Hays, M.; Smith, N.; Kinsey, J.; Dong, Y.; Kariher, P. Polycyclic aromatic hydrocarbon size distributions in aerosols from appliances of residential wood combustion as determined by direct thermal desorption-GC/MS. *J. Aerosol Sci.* **2003**, *34*, 1061–1084. [CrossRef]
64. Ehrlich, C.; Noll, G.; Kalkoff, W.D.; Baumbach, G.; Dreiseidler, A. PM_{10}, $PM_{2.5}$ and $PM_{1.0}$—Emissions from industrial plants—Results from measurement programmes in Germany. *Atmos. Environ.* **2007**, *41*, 6236–6254. [CrossRef]
65. Simoneit, B.; Schauer, J.; Nolte, C.; Oros, D.; Elias, V.; Fraser, M.; Rogge, W.; Cass, G. Levoglucosan, a tracer for cellulose in biomass burning and atmospheric particles. *Atmos. Environ.* **1999**, *33*, 173–182. [CrossRef]
66. SICAM-Ingeniería. Actualización del Inventario de Emisiones Atmosférica para las Comunas de Temuco y Padre las Casas, Año Base 2017. Technical Report. 2014. Available online: https://planesynormas.mma.gob.cl/archivos/2024/proyectos/6fc_Folio_996_al_1173_Informe_Final_Inv._Emisiones_Tco_y_PLC_2020.pdf (accessed on 4 December 2018).
67. Cohen, A.J.; Brauer, M.; Burnett, R.; Anderson, H.R.; Frostad, J.; Estep, K.; Balakrishnan, K.; Brunekreef, B.; Dandona, L.; Dandona, R.; et al. Estimates and 25-year trends of the global burden of disease attributable to ambient air pollution: An analysis of data from the Global Burden of Diseases Study 2015. *Lancet* **2017**, *389*, 1907–1918. [CrossRef]

Disclaimer/Publisher's Note: The statements, opinions and data contained in all publications are solely those of the individual author(s) and contributor(s) and not of MDPI and/or the editor(s). MDPI and/or the editor(s) disclaim responsibility for any injury to people or property resulting from any ideas, methods, instructions or products referred to in the content.



https://dspace.org/

A baseline assessment of residential wood burning and urban air quality in climate-vulnerable chilean cities

Baettig, Ricardo; Ingram, Ben

2025-10-01
MDPI
https://doi.org/10.3390/urbansci9100426
Baettig R, Ingram B. (2025) A baseline assessment of residential wood burning and urban air quality in climate-vulnerable chilean cities. Urban Science, Volume 9, Issue 10, October 2025, Article number 426

Downloaded from a DSpace repository. https://dspace.org/